Quantum transport in a corrugated one-dimensional quantum wire

KyoungWan Park, Seongjae Lee, Mincheol Shin, Jong Seol Yuk, and El-Hang Lee

Research Department, Electronics and Telecommunications Research Institute, Yusong P.O. Box 106, Taejon 305-600, Korea

Hyuk Chan Kwon

Superconducting Division, Korea Research Institute of Standards and Science, Yusong P.O. Box 102, Taejon 305-606, Korea

We report on investigations of the resonant transmission effect of electrons induced by the corrugation of the conducting channel in a gated quantum-wire structure. The corrugation consisted of a periodic indentation of the side wall by which electron waves are scattered backward in the channel. The low-temperature conductance shows a number of peaks in the gate-voltage range where the electron transport is one dimensional. We attribute the resonances to the multiple reflection effect that is interpreted by a simple interference condition. [S0163-1829(98)02628-9]

Quantum interference of phase coherent electrons in semiconductor heterostructures has provided a wealth of interesting physics and devices.[1] For example, many studies of the quantum interference have been reported that show effects associated with double-slit interference,[2] multiple transmission,[3] and multiple reflections.[4] Electron waveguiding in one-dimensional (1D) semiconductor nanostructures was identified through the observation that the conductance in quantum point contacts is quantized at discrete values of $2e^2/h$.[5] The conductance quantization originates from the quantum confinement effect, i.e., the transverse resonant states in the quasi-1D structure. Longitudinal resonant states are established by a longitudinal quantum confinement potential, such as a double-barrier potential in a resonant tunneling diode. Also, the longitudinal resonant states can be formed by a periodically modulated potential in the 1D conducting wire. The formation of the longitudinal resonant states in an artificial 1D crystal allows not only a demonstration of an energy-band structure in solid-state physics but also offers potential applications in quantum devices.

Recently, formation of an energy-band structure in an artificial 1D crystal was investigated experimentally[6] and theoretically.[7] Kouwenhoven *et al.* studied the magnetotransport properties of a channel with a periodically modulated width.[6] The 1D channel was defined by a split gate in their experiment; one gate electrode was straight, but the other gate electrode was corrugated with 15 notches in it. Miniband formation analogous to minibands in superlattice structures was discussed for the conductance oscillations in the voltage range of the straight gate. However, the changes of the gate voltage in the 1D conducting wire formed by a split gate influence the energy of the transverse modes as well as the Fermi energy.[8] Therefore, effects related with the modification of the transverse modes have to be considered in the miniband formation.

In this experiment, we spectroscopically investigated the formation of the longitudinal resonant states in a 1D field-effect-transistor-type conducting wire, such that the gate voltage controls only the Fermi energy. We report on the fabrication of a corrugated 1D conducting wire with a metal gate covering the whole conducting wire. Low-temperature conductance properties induced by the corrugations are described. The longitudinal resonant states are discussed based on the multiple transmission condition.

To investigate the longitudinal resonant states with regard to conductance properties, conducting wire structures with and/or without the periodically corrugated side wall were fabricated. The corrugated conducting wire sample is schematically shown in Fig. 1(a). As a first step, the conducting path of the two-dimensional electron gas (2DEG) was fabricated using electron-beam lithography and subsequent chemical etching on a modulation-doped GaAs/Al$_x$Ga$_{1-x}$As ($x=0.3$) heterostructure grown by molecular-beam epitaxy. The length of the conducting path is 4.0 μm, the width is 0.8 μm in the lithographic length, and the distance between the source and drain Ohmic contacts is 0.6 μm. The heterostructures were wet etched down to the 2DEG layer to form a well-shaped pathway. Lateral depletion further reduces the conducting width. Ni/AuGe/Au metallization and rapid thermal annealing processes were performed in order to make Ohmic contacts in the source and drain regions. As a second step, the gate was fabricated on the conducting path using electron-beam lithography and lift-off technique. This second step defined the Au/Ni gate with the periodically corrugated part in the corrugated wire sample and the strip gate in the normal sample. Then electron-beam lithography and chemical beam assisted ion-beam etching techniques were used to define the etching area and to fabricate the corrugated wire structure. At this moment, we used the corrugated metal gate as an etching mask. Part of the conducting path outside of the corrugated metal gate was dry etched down to the 2DEG layer again. Finally, a periodically corrugated potential wall was formed within the conducting path. The corrugation consists of four notches whose width and separation are about 50 and 160 nm, respectively. The metal gate length is 4 μm, and the metal gate covers the whole conducting area of the wire.

The carrier concentration and mobility in the substrate at 1.5 K were deduced from the Shubnikov–de Haas oscillation measurements in a two-dimensional bar (50×150 μm). They were found to be $n=3.2\times10^{11}$ cm^{-2} and $\mu=5.5\times10^5$ cm^2 V^{-1} s^{-1}, respectively. We measured the conductance σ
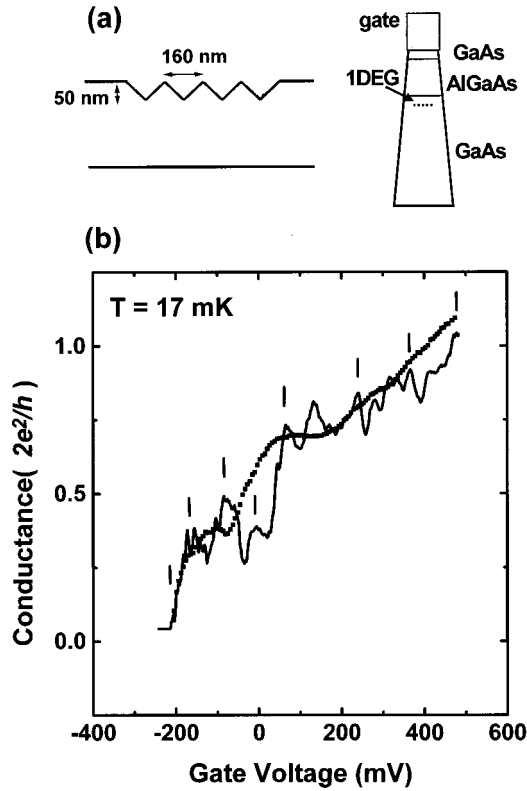
FIG. 1. (a) Schematic diagram of the corrugated conducting path (top view). The metal gate covered the whole conducting wire. For details see the text. Also shown in the right is the cross-sectional view of the 1D quantum wire. (b) Conductance spectra versus the applied gate voltages. The line curves represent the conductance of the corrugated quantum wire; the positions (|) of the major peaks were used for the calculation of the resonant transmission mode index, while the dotted curve represents the conductance of the normal quantum wire without the corrugations.

FIG. 2. Plots of conductances as a function of the gate voltage V_G for several values of the drain voltage V_{DS}. The conductances are shifted by one conductance unit, and some curves show retraces in the gate-voltage sweep for the reproducibility.

and the drain current I_{DS} as a function of applied gate voltages V_G at various levels of drain voltages V_{DS} by using the lock-in technique at 17 mK. The measured drain currents were calibrated as the constant drain bias condition by considering the effect of conductance change during the gate-voltage sweep. We also investigated the temperature dependence of the drain current.

Figure 1(b) shows conductance spectra in the gate-voltage range for both types of devices. The drain current was fixed at 1 nA to minimize the bias heating effects. The pinch-off voltage of both devices is −210 mV. The conductance in the device without the corrugation changes smoothly and a major plateaulike feature is observed at $V_G = \sim 100$ mV: the plateaulike feature also exists in the device with corrugation. The small discrepancy between the measured value and the unit conductance ($2e^2/h$) in the plateau region can be attributed to the extra resistance outside of the gate region. Since conductance steps are typically predicted in 1D quantum wires, the results of Fig. 1(b) demonstrate that our samples are ballistic quasi-one-dimensional quantum wires with one transverse mode in the gate-voltage range. The conductance steps originate from electrical depopulation of the conducting modes by the gate-voltage change. In contrast, large oscillatory features with, e.g., an intensity of ~40% at −80

mV gate voltage, are clearly seen in the device with corrugation. Since these oscillatory behaviors are observed in the corrugated device but not in the normal device, we believe that they are manifestations of the electron multiple transmission effect due to the corrugation. Major peaks can be attributed to the resonant maxima in the multiple transmission spectra, so that we marked the reasonably big peaks with a bar as major peaks, whose positions will be used in the calculation of the resonant transmission mode index in Fig. 4 (how to decide the major peaks will be explained later). Distances between the major peaks are almost equal to ~80 mV in a negative gate-voltage range and ~120 mV in positive gate-voltage range, respectively. Three minor peaks also appear between the major peaks.

We measured the drain currents at various drain bias voltages from 10 μV to 2 mV, then calculated the conductance spectra shown in Fig. 2. Also, the transconductance versus the gate voltage for $V_{DS} = 10$ μV (not shown in this paper) was calculated. Thereby multiple negative transductance oscillations could be seen in the negative slope regions in the curve of the drain current versus the gate voltage. The oscillatory behavior of the conductance persists up to $V_{DS} = 100$ μV, whose intensities are almost constant in this range. In higher drain bias voltages the characteristic oscillations start to smear out until they completely disappear at about 1.2 mV. The change of the oscillation intensity as a function of the drain bias voltage, for example, at $V_G = 66$ mV, is demonstrated in Fig. 3. Measurements of the temperature dependence of the oscillatory behavior reflect how the energy averaging effect reduces the oscillation intensities by the operating temperature in the same way as by the drain bias voltage. No oscillation signals with respect to the gate voltage were detected at temperatures above 1.4 K. However, the signals of the oscillations appeared below 1.06 K with almost constant intensities down to 17 mK. These characteristic behaviors in both the drain bias voltages and the operating temperatures agree well with the results of the typical

(a)

T = 17 mK

V_G = 66 mV

[Plot: ΔG ($2 e^2/h$) vs V_{DS} (μV)]

(b)

V_{DS} = 10 μV

V_G = - 83 mV

[Plot: ΔG ($2 e^2/h$) vs T(K)]
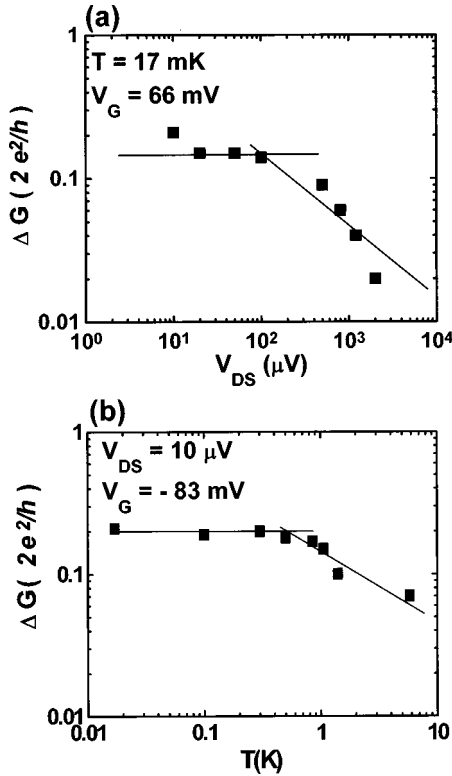
FIG. 3. Conductance changes of the oscillatory intensity as a function of the drain voltage (a) and the operating temperature (b).

[Plot: m (calculated index) vs n (integer)]

FIG. 4. Calculated resonant transmission mode indices, m, $m = 2b/\lambda_F(V_G)$, versus integer number n.

electron interference effect.[9] The results for the correlation energy of the sample system ~ 100 μeV obtained by two different measurements agree well.

Since the electron transport is one dimensional in the sample devices, the electron transport can be strictly described by a plane wave. The gate voltages alter the electron density in the device so that the Fermi wavelength is changed according to $\lambda_F = 4/n_l$ (n_l is the one-dimensional electron density). Then, we observe the multiple transmission spectra with respect to the gate voltage. If we assume that the notch induces backscattering of the electron wave in the corrugated channel, the multiple transmission assumption for the electron transport is rigorously valid. The multiple transmission assumption yields the condition for the maximum conductance: $m\lambda_F = 2lb$, where m is a transport mode index in multiple transmission, l is the number of notches, and b is the separation between notches. This condition establishes the longitudinal transport states in the presence of the corrugations. These states correspond to the maxima in the conductance spectra. Among these states, we will take account of some resonant states, which arise from the minimum segment in the multiple transmission ($l = 1$).

By assuming the multiple transmission due to the corrugation, we theoretically calculated the gate voltages for the resonant transmission. Comparing the experimental data of peak positions in Fig. 1(b) with the calculated ones, some experimental peaks were not considered as a major peak because of large discrepancies from the calculated values. For example, the peak at $V_G = 190$ mV was not assigned as a major peak even though it was rather big.

In Fig. 1(b), those conductance maxima represented by bars are seen to coincide with the peak positions predicted by
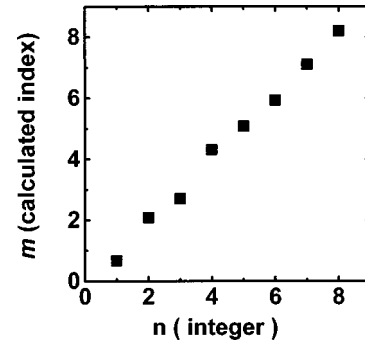
the resonant transmission condition. In order to verify that the observed oscillations are indeed due to the electron resonant transmission, the resonant transmission mode indices, $m = 2b/\lambda_F(V_G)$, are calculated from the peak positions in the gate voltage. They are seen to agree well with the integer multiples. The calculated index values m are plotted against integer numbers n in Fig. 4. We calculated the one-dimensional electron densities at a given gate voltage by considering the conductance spectra of the normal sample without the corrugations (note that the conductance is proportional to the electron density). The electron-density dependence on the gate voltage was included in the calculation of the Fermi wavelength. However, small deviations of the calculated value m from integer n appear for low indices, i.e., for low gate bias voltage above the pinch-off voltage. Irregularities in the conducting width were inevitable in the sample preparation. These create a broadening of the Fermi wavelength in the one-dimensional transport, rendering the value of the Fermi wavelength more uncertain in the ranges of the gate voltage between the conductance steps. Thus, the deviations for low indices are attributed to the uncertainty of the Fermi wavelength induced by the irregularities in the conducting width.

It should be noted that the multiple transmission effect due to the periodically corrugated potential wall in the one-dimensional transport gives rise to the secondary maxima with respect to the wavelength, that is, with respect to the applied gate voltage in the conductance measurement. We observed approximately three secondary maxima between the principal maxima, which could be explained by the resonant transmission condition due to the larger segments; $l = 2$, 3. This result is in accordance with the number (4) of notches: that is, there are three minimum segments for the backscattering of electrons in the corrugated potential wall sample.

A periodic potential forms an energy-band structure characterized by energy bands and separated by energy gaps in collective states. Recently, formation of the energy gap and the miniband in an artificial one-dimensional crystal was reported.[6] The crystal consisted of a sequence of quantum dots defined by a finger-type split gate to form a corrugated ballistic channel. Although the negative gate bias voltage simultaneously reduced the coupling between adjacent dots, reduced the area of each dot, and lowered the Fermi energy in their experiments, the magnetoconductance oscillations could be correctly interpreted as formations of the minibands

with the energy gaps in terms of resonant transmission. Since the gate voltage controls the Fermi energy in our sample structure, the formation of the longitudinal resonant states can be quantitatively explained by the multiple transmission conditions. On the other hand, due to the *open* conduction between the indentations, it is difficult in the corrugated quantum wire to observe a set of nicely formed minibands representing Bloch states.[10] However, the conductance spectra of Fig. 1(b) exhibit not only peaks for the individual resonant states but also valleys between the states, which can be associated with energy gaps.

In summary, we investigated the electrical transport properties of a $GaAs/Al_xGa_{1-x}As$-based quantum wire transistor containing a periodically corrugated potential wall in the conducting path. In contrast to the one-dimensional crystal formed by the split gate, only the Fermi energy was controlled by the gate voltage in the device. The longitudinal resonant states were observed spectroscopically. A multiple transmission assumption was shown to account quantitatively for the conductance oscillations.

---

[1] Many references can be found in *Nanostructure Physics and Fabrication*, edited by M. A. Reed and W. P. Kirk (Academic, Boston, 1989).

[2] G. Cernicchiaro, T. Martin, K. Hasselbach, D. Mailly, and A. Benoit, Phys. Rev. Lett. **79**, 273 (1997); H. Hongo, Y. Miyamoto, K. Furuya, and M. Suhara, Appl. Phys. Lett. **70**, 93 (1997); K. Park, S. Lee, M. Shin, E-H. Lee, and H. C. Kwon, Phys. Rev. B **54**, 1498 (1996).

[3] K. Tsubaki, T. Honda, H. Saito, and Y. Tokura, Appl. Phys. Lett. **58**, 376 (1991).

[4] J. C. Wu, M. N. Wybourne, W. Yindeepol, A. Weisshaar, and S. M. Goodnick, Appl. Phys. Lett. **59**, 102 (1991).

[5] B. J. van Wees, H. van Houten, C. W. J. Beenakker, J. G. Williamson, L. P. Kouwenhoven, D. van der Marel, and C. T. Foxon, Phys. Rev. Lett. **60**, 848 (1988).

[6] L. P. Kouwenhoven, F. W. J. Hekking, B. J. van Wees, C. J. P. M. Harmans, C. E. Timmering, and C. T. Foxon, Phys. Rev. Lett. **65**, 361 (1990).

[7] M. Leng and C. S. Lent, Phys. Rev. Lett. **71**, 137 (1993); C. S. Lent and M. Leng, Appl. Phys. Lett. **58**, 1650 (1991).

[8] G. Timp, in *Nanostructured Systems*, edited by M. Reed (Academic, Boston, 1992), p. 113.

[9] F. P. Milliken, S. Washburn, C. P. Umbach, R. B. Laibowitz, and R. A. Webb, Phys. Rev. B **36**, 4465 (1987).

[10] The authors of Ref. 6 formed a 1D individual quantum-dot array by the finger-type split gate in which the coupling between the dots was weak enough for new minibands to form easily in the sample. However, in our corrugated quantum wire electron waveguiding was the dominant transport mechanism, because most resonant peaks in these gate-voltage ranges had conductances not far from the value at the conductance plateau. Hence, we considered the resonant transmission effect in the original conduction mode instead of a new formation of the miniband.